ACS OMEGA

http://pubs.acs.org/journal/acsodf

Article

Simple Setup Miniaturization with Multiple Benefits for Green Chemistry in Nanoparticle Synthesis

Jette K. Mathiesen,[§] Susan R. Cooper,[§] Andy S. Anker, Tiffany L. Kinnibrugh, Kirsten M. Ø. Jensen,* and Jonathan Quinson*

Cite This: *ACS Omega* 2022, 7, 4714−4721

Read Online

ACCESS | Metrics & More | Article Recommendations | Supporting Information

ABSTRACT: The development of nanomaterials often relies on wet-chemical synthesis performed in reflux setups using round-bottom flasks. Here, an alternative approach to synthesize nanomaterials is presented that uses glass tubes designed for NMR analysis as reactors. This approach uses less solvent and energy, generates less waste, provides safer conditions, is less prone to contamination, and is compatible with high-throughput screening. The benefits of this approach are illustrated by an *in breadth* study with the synthesis of gold, iridium, osmium, and copper sulfide nanoparticles.

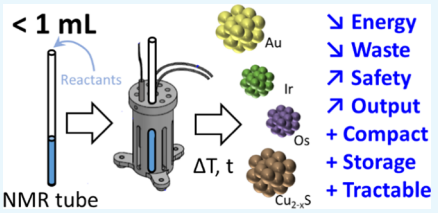

INTRODUCTION

Nanomaterials (NMs) are used in multiple applications ranging from catalysis, optics, and medicine to water/air treatments.[1−3] Due to strong structure−property relations on the nanoscale, careful and rational synthesis of NMs is important. Consequently, the controlled synthesis of NMs has been increasingly addressed as a key component of green chemistry.[4−8] The need for protocols generating less waste and increasing safety has been emphasized.[6,7] Selection of solvents and reactants is often focused upon,[9] and the use of microwaves or ultrasound if considered more energy efficient.[8] The development of setups such as flow (micro)reactors is also useful to minimize waste and simplify NM synthesis.[10−12] However, "despite these advantages, microfluidic systems have yet to be extensively adopted by the colloidal nanomaterial community".[13] The above strategies often require specific equipment and expertise, which may account for their relatively limited implementation. Simpler miniaturized systems with high-throughput potential are to be proposed.

Wet-chemical methods often show promising scalability while being easily implemented in most modern laboratories.[14−16] NMs with various compositions, sizes, and structures can be prepared by wet-chemical synthesis, which results in tuned NM properties to best match specific requirements for various applications.[16−18] The control over NM features is achieved by tuning experimental parameters, e.g., temperature, concentration of reactants, type of reactants, or solvent composition. However, studying and understanding how synthetic parameters influence the NMs produced is often limited by the time and resources required to make a single batch of NMs. In a textbook approach using reflux setups, 10−100 mL of solvents is typically required and only one experiment can be performed every few hours and per setup (see Scheme 1). To understand how NM structures change with synthetic parameters, alternative high-throughput strategies are needed.

Scheme 1. Moving from a *Round-Bottom Flask* to *NMR Tube* Glassware for Greener NM Synthesis and Studies

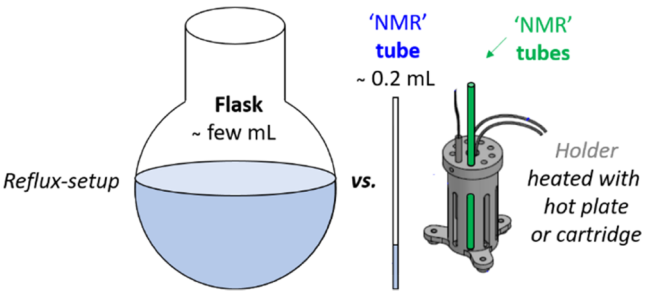

As an alternative to the conventional reflux setup, we here investigate the use of glass tubes designed for nuclear magnetic resonance (NMR) measurements as miniaturized reactors[19,20] (see Scheme 1 and details in the Methods section). Multiple advantages of this simple alternative in green chemistry for NM synthesis[6,8] are illustrated by an *in breadth* study with the preparation of four different nanoparticles (NPs): gold (Au), iridium (Ir), osmium (Os), and copper sulfide ($Cu_{2-x}S$). Although precious metal (PM)-based NPs are made of nonrenewable resources, they remain key materials in multiple applications,[7] e.g., to develop fossil fuel-free technologies for

Received: January 3, 2022
Accepted: January 17, 2022
Published: January 25, 2022

energy conversion,[17] and as models to understand NM formation.[21] Even minor improvements in PM NP synthesis can have significant scientific, economic, and ecological impacts.

RESULTS AND DISCUSSION

Au NPs. Au NPs have been a case study for green chemistry in NM synthesis.[7] In particular, the Turkevich synthesis is widely reported, where, typically, 0.1−0.5 mM $HAuCl_4$ is reduced in water close to the boiling point by trisodium citrate.[22,23] The investigation of many parameters controlling the properties of Au NPs[22] would gain from high-throughput approaches using less solvent than the typical 200−500 mL required. The Au NPs obtained performing the Turkevich synthesis in 500 mL (reflux setup) or 0.2 mL (NMR tube) lead to the same NP size, ca. 13 nm within the error of measurement, by TEM (Figure 1). A range of alternative Au

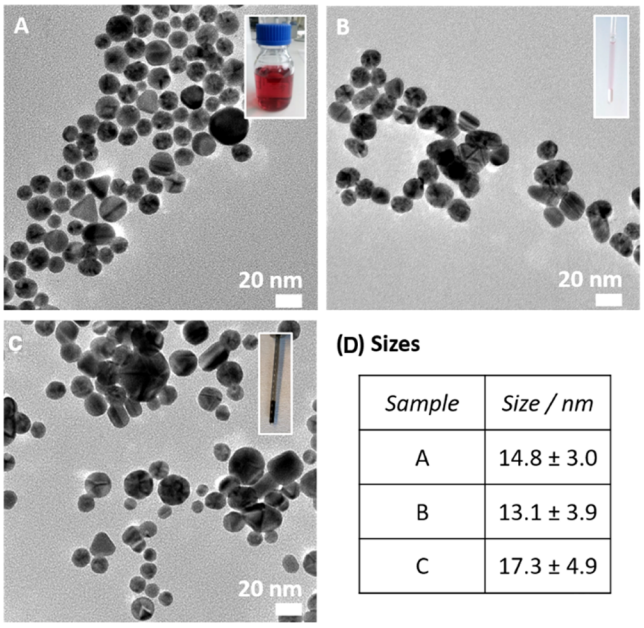

(D) Sizes

Sample	Size / nm
A	14.8 ± 3.0
B	13.1 ± 3.9
C	17.3 ± 4.9

Figure 1. TEM micrographs of Au NPs obtained from 0.125 mM $HAuCl_4$ in water in the presence of 2.2 mM trisodium citrate at 100 °C for 1 h for a total volume of (A) 500 mL and (B) 0.2 mL. (C) TEM micrographs of Au NPs obtained using oleylamine at 200 °C as a solvent in 0.3 mL. Insets are pictures of the resulting colloidal dispersions. TEM micrographs acquired at different magnifications and the related size distributions are available in Figure S1. (D) Table of the related size distributions.

NP syntheses use organic solvents, such as oleylamine, at relatively high temperatures.[24] Syntheses at higher temperatures, e.g., 200 °C, are possible since nuts and ferrules can be used to close the NMR tube (Figure 1C).

Ir NPs. We reported a surfactant-free colloidal synthesis of PM NPs directly relevant for the industry,[17,25] performed at low temperatures (<80 °C) in alkaline monoalcohols like methanol or ethanol, leading to high catalytic activity for the oxygen evolution reaction,[17,26] without intensive washing or purification steps, thus already addressing few green chemistry principles for NP synthesis.[6,7,27] The Ir NPs are in the range 1−2 nm across a wide range of experimental parameters.[28] To possibly achieve size control, investigating high concentrations of precursors and long synthesis time are reasonable options. Using a microwave or even a classical reflux setup, it is arguably challenging to investigate these hypotheses due to safety concerns, higher precursor cost and pressure on lab space as well as equipment access.

Using NMR tubes, safe and simple time-resolved studies over weeks of synthesis at high precursor concentrations (100 mM $IrCl_3$) are easily performed (see Figure 2). In line with

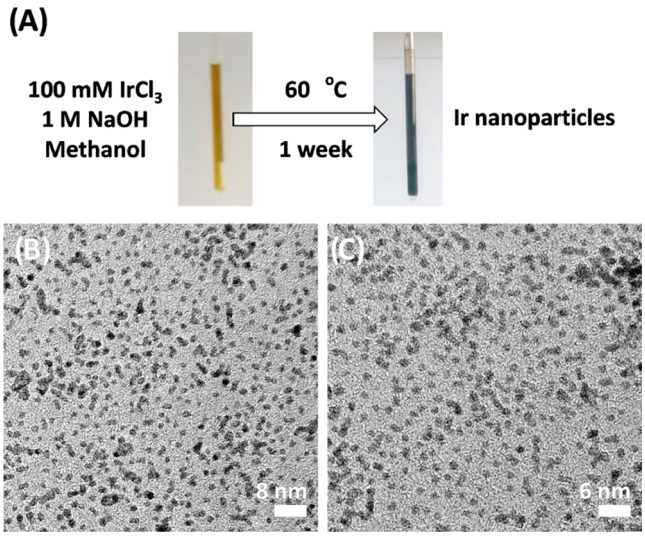

Figure 2. (A) General conditions for Ir NP synthesis. The NMR tube is 3 mm in diameter and the magnetic stirrer bar is 1.5 mm long. (B, C) TEM micrographs at different magnifications of Ir NPs obtained from 100 mM $IrCl_3$ in 1 M NaOH in methanol at 60 °C for a week for a total volume of 0.2 mL (see also Figures S2 and S3).

previous reports using microwave synthesis[17] or UV−vis-induced synthesis,[28] it is found that Ir NPs with an average size of 1.6 nm are obtained. A significant achievement here is that the NPs are obtained at high concentrations (100 mM) of precursors. This result underlines the relevance of this recently reported Ir NP synthesis to scale up the synthesis of extremely active catalysts for the oxygen evolution reaction.[17,29]

Os NPs. Os NP synthesis has received less attention than other PMs.[30−32] Taking advantage of the small volume of solvent needed, we investigated the surfactant-free synthesis of Os NPs at a high precursor concentration in simple low boiling point solvents such as a mixture of methanol and water. TEM micrographs of the resulting materials obtained for a one-week long synthesis starting with 100 mM of $OsCl_3$ show that small-sized NPs, ca. 1.6 ± 0.4 nm in diameter, are obtained (Figure 3). Although Os NPs are made of non-earth-abundant elements, the small-sized Os NPs obtained by a surfactant-free approach are relevant to develop more sustainable energy conversion systems to move away from fossil-fuel-based energy.[33−35]

$Cu_{2-x}S$ NPs. $Cu_{2-x}S$ NPs have applications in batteries,[36,37] sensors,[38] and as an oxygen reduction reaction catalyst.[39] The analysis with a lab-source XRD instrument of the NPs synthesized in the NMR tubes suggests that small $Cu_{2-x}S$ NPs are formed (Figure 4A). TEM analysis shows a size of 4.5 ± 0.9 nm (Figures 4B and S5). While some features are observed in the XRD pattern in Figure 4A, the broadening of Bragg peaks from these small NPs makes any structural investigation challenging. In contrast, the use of the NMR tube makes further characterization straightforward, e.g., using

https://doi.org/10.1021/acsomega.2c00030
ACS Omega 2022, 7, 4714−4721

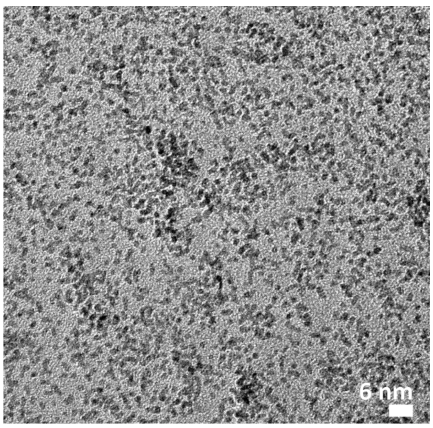

Figure 3. TEM micrographs of Os NPs obtained from 100 mM $OsCl_3$ in methanol/water (1:2, v-v) at 85 °C for a week for a total volume of 0.2 mL. Size distribution is available in Figure S4.

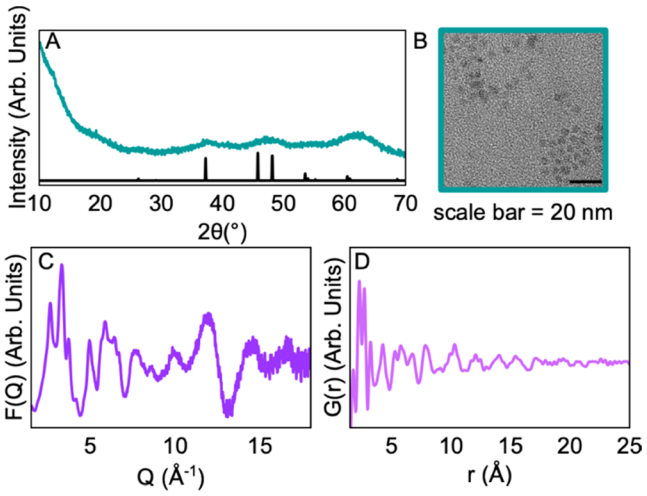

Figure 4. Characterization of $Cu_{2-x}S$ NPs obtained in an NMR tube setup. (A) Using a lab-source XRD instrument (blue) compared to a calculated diffraction pattern of β-chalcocite taking the space group $P63/mmc$ (black). (B) TEM micrographs of the washed NPs. (C) F(Q) and (D) PDF ($G(r)$) of X-ray total scattering data.

synchrotron scattering techniques, as many measurements can be done directly on the sample in the NMR tube. For instance, the as-prepared samples in closed NMR tubes can be sent to synchrotron for X-ray total scattering with pair distribution function (PDF) analysis. The PDF can be understood as a histogram of atom−atom distances in the material. Figure 4C,D shows the $F(Q)$ (data in reciprocal space) and $G(r)$ (data in real space) of the reaction solution after background subtraction. The PDF analysis confirms that the NPs can be described by a β-chalcocite model in the space group $P63/mmc$[40] with deviations in the local structure (Figure S6). Furthermore, the structure obtained is the same whether the reaction is performed in the NMR setup or a conventional reflux setup.

Benefits. The use of NMR tubes readily leads to several advantages in terms of synthesis strategy. The syntheses with volume as low as 0.1 mL are feasible using 3 mm-diameter-NMR tubes (Figure 2). This low volume reduces the amount of waste generated and allows investigating the effect of high concentration solutions toward scaling up.[7,16] Sample holders can be designed to perform several experiments at a time (up to 9 experiments per holder in the current design, Figure S7), allowing high-throughput screening while requiring minimal lab space. Small volume also allows safer operating conditions. As a result, both long(er) and an increased number of experiments can be performed with few pieces of equipment while optimizing the energy needed to heat up the solutions. Temperature control is achieved by either using the temperature control of a heating plate or using a dedicated heating cartridge with a temperature controller to control the heating rate (Figure 5 in the Methods section). Septa can be used to close the NMR tubes to control the atmosphere; alternatively, nuts and ferrules can be used for higher pressure experiments. The length of the NMR tube provides an area of contact with cool air to function under reflux conditions. This area can also be cooled, e.g., with a fan or dedicated water-cooling devices. It is worth emphasizing that the synthesis can be performed with stirring by simply using a commercially available stirrer bar (e.g., 8 mm × 1.5 mm) in the NMR tube (Figure 2).

Further Considerations. NMR tubes have previously been used as reactors for *in situ* studies at synchrotrons or for

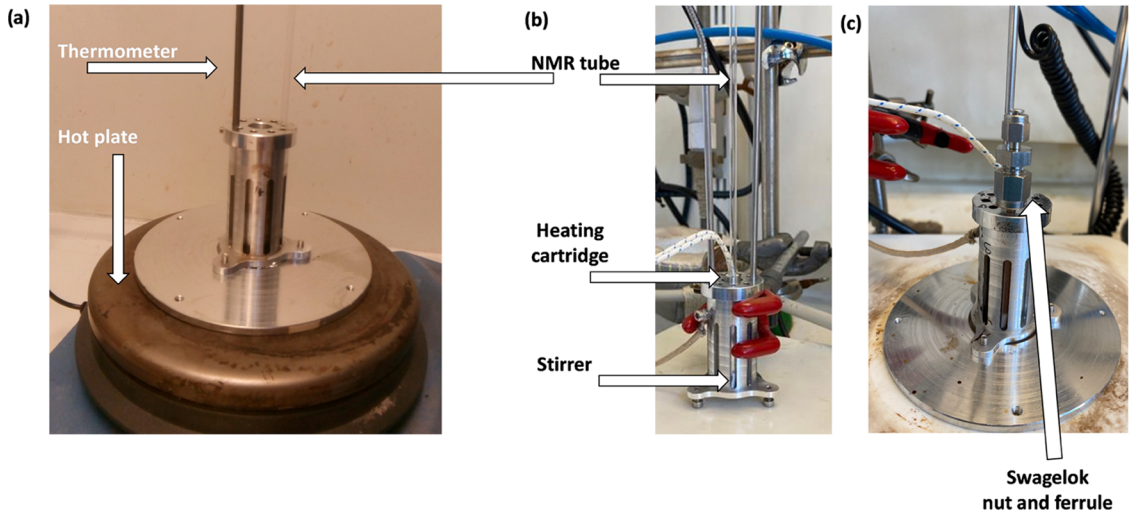

Figure 5. Photographs of different setups using a 3 mm NMR tube as a reaction vessel (a) using a hot plate, (b) using a heating cartridge, and (c) using a Swagelok nut and ferrule. The stirrer bar is 1.5 mm long, and the NMR tube is 3 mm in diameter. See technical details in Figure S7.

https://doi.org/10.1021/acsomega.2c00030
ACS Omega 2022, 7, 4714−4721

NMR characterization.[20,41] However, they have often been used to make the experiment compatible with a given type of measurement, e.g., NMR, and not as a preferred reaction vessel. The experimental conditions selected to perform these specific experiments are often the results of screening performed on larger-scale syntheses. A drawback of screening studies developed and optimized in laboratories is that they are often challenging to directly adapt to the requirements and limitations of dedicated characterization setups. For example, PDF measurements are best performed on samples with a high concentration of the material of interest, especially when considering poorly scattering elements like transition metal sulfides. Here, the NMR tube setup offers the option to readily investigate a high concentration of materials during parametric studies performed in home laboratories (outside synchrotrons facilities). Ultimately, this allows comparing more directly selected measurements performed at synchrotron facilities with larger screening experiments done in a chemistry lab. This further enables researchers to design experiments for even more complex *in situ* analysis of various reactions.[19,41,42]

NMR tubes make it possible to use a clean vessel for each experiment. This alleviates the need to clean glassware, thus limiting the chemical waste generation related to cleaning steps, e.g., using *aqua regia* for Au NPs.[43] Importantly, it alleviates the question of cross-contamination, thus addressing the well-known issue of reproducibility in NM science, often ascribed to chemical impurities from various sources.[44] NM synthesis can be sensitive to variations of room temperature or room light, and the stability over time of the chemicals and/or precursor solutions can be an issue.[45] These variables may be challenging to control across long periods of time when a study would last, for instance, several weeks or months. This drawback is alleviated with NMR tubes as reactors since several experiments including controls can be performed at the same time. Energy is saved because several experiments are heated all at once. The ease of simply performing relatively long experiments is also a positive feature toward the improved yield of the precursor conversion to NMs.

It could be argued that due to the small diameter of the NMR tubes, capillary effects might come into play and the actual temperature−pressure during the reaction might not be well known. This issue of variability in physical parameters of reactors, e.g., heat transfer properties, stirring, etc., is the same for most scaling up to date, e.g., when moving from reflux setups to larger-scale reactors. In this respect, the use of NMR tube reactors remains a convenient and *green* approach to (pre)screen the influence of experimental parameters.

A final practical consideration is storage and reuse. The small NMR tubes are easily stored due to their small diameter and length. The 18 cm long NMR tube are easily cut with a commercially available glass cutter to save more space. The open end of the glass can be sealed by melting with a torch (e.g., butane torch), for instance, when toxic reagents and/or air-sensitive compounds are involved. The samples can be safely and space-efficiently stored for further analysis. Additionally, the cut section of the NMR tube can be cleaned and sealed by melting one extremity to be reused as a new miniaturized vessel.

CONCLUSIONS

A simple alternative to the classical round-bottom flask synthesis approach to prepare NMs is presented. An *in breadth* study of four different nanomaterials is presented, covering gold, iridium, osmium, and copper sulfide nanomaterials. The general approach is relevant for the synthesis of other nanomaterials like palladium, platinum, or silver that would be performed in similar solvents and/or for the same temperature range.[17,46] Using commercially available NMR tubes, a miniaturized vessel suitable for the synthesis of various NMs is readily obtained. This approach complies with many of the principles of green chemistry for NM synthesis.[6,7] This approach is therefore directly relevant not only for academic research and research and development but also for educational purposes.

With the increasing interest in machine learning and artificial intelligence, large datasets are needed to feed algorithms.[47] The present approach allows for high-throughput (pre)-screening. Multitechnique characterization remains a general limiting factor in nanoscience[48] but the expected improvements in this area of research are promising.[6,19,41,49] If characterization is kept minimal in this *in breadth* approach, enough material is still obtained for characterization by TEM, XRD, or PDF and naturally NMR, high-resolution TEM, or UV−vis characterization with an appropriate setup. It is expected that the simple alternative proposed here will also be relevant for various synthesis of molecules and other chemical reactions.

METHODS

Chemicals. All chemicals were used as received: $HAuCl_4 \cdot 3H_2O$ (≥99.9% trace metals basis Merck); trisodium citrate (99%, Alfa Aesar); $IrCl_3$ (99.8%, metals basis, Alfa Aesar); $OsCl_3 \cdot xH_2O$ (Sigma-Aldrich); NaOH (ACS, Reag. EMSURE, Merck); methanol (≥99.9%, HiPerSolv Chromanorm, VWR); water (Milli-Q, Millipore, resistivity > 18.2 MΩ·cm, total organic carbon (TOC) < 5 ppb); oleylamine (OLA, 70%, technical grade, Sigma-Aldrich); gold(III) acetate ($Au(ac)_3$, 99.9% metal basis, Alfa Aesar); 1-dodecanethiol (>98%, Sigma); *n*-hexane (≥97%, HiPerSolv CHROMANORM, VWR); oleic acid (90% technical grade, Sigma); Cu(II) acetate (99% trace metal basis, Sigma); and acetone (Chemex Products Aps).

Materials. NMR tubes (Wildmad, 3 mm outer diameter, 0.27 mm wall thickness, type 1 class A), magnets (Fisherbrand PTFE stirrer bar, 8 mm × 1.5 mm), and copper or nickel transmission electron microscope (TEM) grids (Quantifoil or Agar Scientific) were all used as received. The synthesis was performed in the configurations detailed below in Figure 5 using a homemade NMR tube holder detailed in Figure S7. It can also be performed by placing the NMR tubes in a temperature-controlled water or oil bath.

Syntheses. *Note*: Some reactions can be dangerous, here, in particular, the synthesis of Os nanoparticles (NPs), since OsO_4 can easily form and is highly toxic. The synthesis must be performed in a fume cupboard. Conveniently, the synthesis can be performed in NMR tubes closed with a cap (red cap provided upon buying the NMR tubes or further septa fitting the NMR tubes can be purchased: Precision seal rubber septa cap (for 3 mm OD tubes and ampoules) pack of 100 ea) and further sealed with parafilm. Alternatively, the NMR tube can be melted and sealed for the experiment or at the end of the experiments, e.g., with a butane torch. Otherwise, nuts and ferrules (Swagelok) can be used. These opportunities to seal the vessel are also relevant for further storage.

Au NP Synthesis. Au NPs were obtained following the general procedure of the Turkevitch synthesis.[22,23] They were

https://doi.org/10.1021/acsomega.2c00030
ACS Omega 2022, 7, 4714−4721

produced from a mixture of 0.125 mM $HAuCl_4$ with 2.2 mM trisodium citrate in water for a total volume of 500 mL in a reflux-setup or 0.2 mL in a 3 mm diameter NMR tube. The solution containing trisodium citrate was preheated at 100 °C before the gold-containing solution was added (the volume before gold injection was 499 mL or 0.1 mL). In both cases, a hot plate was used to heat up the solution to 100 °C and the reaction after adding gold was left for 1 h at this temperature of 100 °C with a stirring rate set at 1000 rotations per minute. The solution initially yellow turns red over time.

Alternatively, Au NPs were obtained using organic solvents.[24,50] To a glass vial, 9 mL of oleylamine (OLA) and 25 mM $Au(ac)_3$ were added. The precursor solution was heated to 50 °C under air while stirring at 400 rotations per minute (rpm) until the metal ion precursor was dissolved. Briefly, 4.5 mL of the precursor solution was taken to a separate vial, into which 25 μL of dodecanethiol (DDT) was added and further heated to 50 °C under air while stirring at 400 rpm. Typically, 0.3 mL of the solution was added to an NMR tube and closed by Swagelok nuts and ferrules. The NMR tube was placed in the heating block, where the solution was heated to 200 °C at a heating rate of 7 °C min^{-1} and maintained at this temperature for 1 h. The solution was cooled to room temperature. The resulting solution was added to a centrifuge tube with 20 mL of hexane and was spun at 10 000 rpm for 10 min to precipitate the NPs. The particles were washed with ethanol/hexane (3:1 ratio) three times. The particles were then suspended in 5 mL of hexane for future use.

Ir NP Synthesis. The Ir NPs were obtained following the general procedure previously reported.[17,26,28] A mixture of 100 mM $IrCl_3$ in 1 M NaOH in methanol for a total volume of 0.2 mL was placed in a 3 mm diameter NMR tube with a magnetic stirrer bar. The filled NMR tube was placed in a dedicated holder as presented in Scheme 1 and Figure 5. A hot plate was used to heat up the miniaturized vessel to 60 °C for up to 1 week with a stirring set at 1000 rotations per minute. The solution, which is initially light brown, turns black over time (see Figure 2).

Note: We previously used 4.4 mM in 10 mL[17] or 27 mL[26] to get enough mass of iridium, 8.5 mg and 23 mg, respectively, for electrochemical testing. Using here ca. 20 times less solvent, the same mass of Ir NPs can be obtained due to the high concentration used.

Os NP Synthesis. The Os NPs were obtained from a mixture of 100 mM $OsCl_3$ in methanol/water (1:2; v-v) for a total volume of 0.2 mL placed in a 3 mm diameter NMR tube with a magnetic stirrer bar. The filled NMR tube was placed in a dedicated holder as presented in Scheme 1 and Figure 5. A hot plate was used to heat up the miniaturized vessel to 85 °C for 1 week with a stirring set at 1000 rotations per minute.

$Cu_{2-x}S$ NP Synthesis. To form copper sulfide NPs, a synthesis reported in the literature was modified.[51] A copper oleate precursor was obtained by heating 1 mmol Cu(II) acetate with 2 mL of oleic acid in an oil bath at 150 °C for 1 h. To 2 mL of copper oleate, 0.2 mL of DDT was added, resulting in a viscous white precipitate. The mixture was mixed using a table-top vortex to ensure solution homogeneity. A mixture of copper oleate and DDT was then added to 9.5 cm × 3 mm NMR tubes (obtained after cutting the initially 18 cm long tubes with a glass cutter) with approximately 0.25 mL using a needle and luer lock syringe. The NMR tubes were filled with N_2 and capped with a 3 mm silicone septa. The bottom of the septa was secured with epoxy and then wrapped in Teflon tape. The NMR tubes were then put into the heating setup equipped with a heating cartridge and a type J thermocouple that were plugged into a Cole parmer Digitroll II temperature controller. The samples were heated with a ramp rate of 185 °C h^{-1} to a final temperature of 200 °C and held at 200 °C for 3 h before being cooled to room temperature.

Two identical samples were prepared in NMR tubes so that three different analyses could be done: lab-source XRD, TEM, and PDF analysis of X-ray total scattering data collected at 11-ID-B at Argonne National Laboratory. Therefore, the NPs in one of the NMR tubes were washed by transferring the reaction liquid using a needle and a luer lock syringe to a 50 mL centrifuge tube. Approximately 5 mL of hexanes was used to rinse the NMR tube to ensure that as much of the reaction liquid as possible was transferred for washing. Acetone was then added to the NMR tube and it was centrifuged for 10 min at 9000 rpm. Particles were redispersed in hexanes and then washed one more time with acetone for 5 min and again with ethanol for 10 min before lab-source XRD and TEM analysis.

Characterization. *TEM Microscopy.* TEM microscopy was performed on a JEOL 2100 operated at 200 kV. The as-prepared or washed Au, Ir, Os, or $Cu_{2-x}S$ NP dispersions were dropped on TEM grids and images recorded in at least three different and randomly selected areas of the grids at least at three different magnifications. The size of the NPs was evaluated by measuring the diameter of at least 100 individual NPs for each sample using the software ImageJ.

Powder X-ray Diffraction. $Cu_{2-x}S$ NPs were dispersed in hexanes and drop cast onto a zero-background substrate for analysis on a Bruker D8 diffractometer with a Cu anode equipped with a Ni filter. The powder diffraction data were collected in Bragg−Brentano geometry from 10 to 70° 2θ.

X-ray Total Scattering Measurements. Data were measured at the 11-ID-B beamline at Argonne National Laboratory. Measurements were done using the beamline mail-in program and remote beamline operation due to the Covid-19 pandemic. The samples were shipped from Copenhagen, Denmark, to Argonne National Laboratory, in the NMR tube closed with a silicone septum, sealed with epoxy and Teflon tape. A sample for subtraction of the signal from the solvent was prepared by mixing 1.8 mL of oleic acid and 0.2 mL of DDT and filled in NMR tubes. The reaction solution, solvent sample, and an empty capillary were placed in an aluminum block for data collection at room temperature. The X-ray wavelength was 0.2115 Å and data were collected using a PerkinElmer detector (200 μm × 200 μm pixel size) with a detector distance of 183.5 mm. Data were collected on the empty capillary, solvent, and sample for 5 min. The data were integrated using Fit2D.[52] The data obtained from the glass capillary were subtracted from the data obtained from the reaction solution and solvent samples before using xPDFsuite,[53,54] to subtract the signal from the solvent from the reaction solution and generate the PDF. The instrument parameters Q_{max} = 18.5 $Å^{-1}$ and 18 $Å^{-1}$, Q_{min} = 1.5 $Å^{-1}$, and r_{poly} = 1.1 were used to generate the PDF.

PDF Refinements. CeO_2 was used for the calibration for the detector distance as well as to determine the Q_{broad} and Q_{damp} parameters of the instrument. The PDF from the CeO_2 standard was modeled in the range from 1.3 to 60 Å with Q_{broad} = 0.0385 $Å^{-1}$ and Q_{damp} = 0.0373 $Å^{-1}$ using the CeO_2 crystal structure model. Modeling of the sample PDF was done using PDFgui and the β-chalcocite structural model in the space group *P*63/*mmc*. The refined parameters are given in

https://doi.org/10.1021/acsomega.2c00030
ACS Omega 2022, 7, 4714−4721

Tables S1 and S2. Two refinements were done at two different r-ranges. The first was done using the chalcocite structural model refined to the PDF in the range 2 to 30 Å (Table S1). The second was done using the chalcocite structural model refined to the PDF in the range 5.6 to 30 Å. The delta2 parameter (describing correlated motion) and $sp_{diameter}$ were fixed at values refined in the first refinement (Table S2).

■ ASSOCIATED CONTENT

Supporting Information

The Supporting Information is available free of charge at https://pubs.acs.org/doi/10.1021/acsomega.2c00030.

The following files are available free of charge. TEM and PDF characterization; sample holder specification; Figures S1−S7, further discussion (PDF)

■ AUTHOR INFORMATION

Corresponding Authors

Kirsten M. Ø. Jensen − *Chemistry Department, University of Copenhagen, 2100 Copenhagen, Denmark;* orcid.org/0000-0003-0291-217X; Phone: +45 35 33 47 97; Email: kirsten@chem.ku.dk

Jonathan Quinson − *Chemistry Department, University of Copenhagen, 2100 Copenhagen, Denmark;* orcid.org/0000-0002-9374-9330; Email: jonathan.quinson@chem.ku.dk

Authors

Jette K. Mathiesen − *Chemistry Department, University of Copenhagen, 2100 Copenhagen, Denmark*

Susan R. Cooper − *Chemistry Department, University of Copenhagen, 2100 Copenhagen, Denmark;* orcid.org/0000-0002-1608-6713

Andy S. Anker − *Chemistry Department, University of Copenhagen, 2100 Copenhagen, Denmark;* orcid.org/0000-0002-7403-6642

Tiffany L. Kinnibrugh − *X-ray Science Division, Advanced Photon Source, Argonne National Laboratory, Argonne, Illinois 60439, United States*

Complete contact information is available at: https://pubs.acs.org/10.1021/acsomega.2c00030

Author Contributions

§J.K.M. and S.R.C. contributed equally to this work. The manuscript was written through contributions of all authors. All authors have given approval to the final version of the manuscript.

Funding

This project has received funding from the European Union's Horizon 2020 research and innovation program under the Marie Sklodowska-Curie grant agreement No. 840523 (CoSolCat, JQ) and 841903 (SRC). This project has received funding from the Villum Foundation through a Villum Young Investigator grant (VKR00015416) and the Danish National Research Foundation (DNRF 149) Center for High-Entropy Alloy Catalysis (CHEAC). This research used resources of the Advanced Photon Source, a U.S. Department of Energy (DOE) Office of Science User Facility, operated for the DOE Office of Science by Argonne National Laboratory under Contract No. DE-AC02-06CH11357 (GUP-73929).

Notes

The authors declare no competing financial interest.

■ ACKNOWLEDGMENTS

E.T.S. Kjær, B. Wang, O. Aalling-Frederiksen, R. Pittkowski, University of Copenhagen, Denmark, H-C. Lu, University of Texas at Austin, USA, and beamline scientists O.J. Borkiewicz and L.C. Gallington are thanked for their help on synchrotron beamtime. S.B. Simonsen and L. Theil Kuhn, Technical University of Denmark, Denmark, are thanked for access to TEM facilities. Morten Liborius Jensen from the University of Copenhagen workshop is thanked for his help on the cell holder design and manufacturing.

■ REFERENCES

(1) Cargnello, M. Colloidal nanocrystals as building blocks for well-defined heterogeneous catalysts. *Chem. Mater.* **2019**, *31*, 576−596.

(2) Kalus, M. R.; Rehbock, C.; Barsch, N.; Barcikowski, S. Colloids created by light: Laser-generated nanoparticles for applications in biology and medicine. *Mater. Today: Proc.* **2017**, *4*, S93−S100.

(3) Chaudhary, S.; Sharma, P.; Chauhan, P.; Kumar, R.; Umar, A. Functionalized nanomaterials: a new avenue for mitigating environmental problems. *Int. J. Environ. Sci. Technol.* **2019**, *16*, 5331−5358.

(4) Schmidt, J.; Marques, M. R. G.; Botti, S.; Marques, M. A. L. Recent advances and applications of machine learning in solid-state materials science. *Npj Comput. Mater.* **2019**, *5*, 1−36.

(5) Dhand, C.; Dwivedi, N.; Loh, X. J.; Ying, A. N. J.; Verma, N. K.; Beuerman, R. W.; Lakshminarayanan, R.; Ramakrishna, S. Methods and strategies for the synthesis of diverse nanoparticles and their applications: a comprehensive overview. *RSC Adv.* **2015**, *5*, 105003−105037.

(6) Hutchison, J. E. The road to sustainable nanotechnology: Challenges, progress and opportunities. *ACS Sustainable Chem. Eng.* **2016**, *4*, 5907−5914.

(7) Gilbertson, L. M.; Zimmerman, J. B.; Plata, D. L.; Hutchison, J. E.; Anastas, P. T. Designing nanomaterials to maximize performance and minimize undesirable implications guided by the Principles of Green Chemistry. *Chem. Soc. Rev.* **2015**, *44*, 5758−5777.

(8) Duan, H. H.; Wang, D. S.; Li, Y. D. Green chemistry for nanoparticle synthesis. *Chem. Soc. Rev.* **2015**, *44*, 5778−5792.

(9) Prat, D.; Wells, A.; Hayler, J.; Sneddon, H.; McElroy, C. R.; Abou-Shehada, S.; Dunn, P. J. CHEM21 selection guide of classical- and less classical-solvents. *Green Chem.* **2016**, *18*, 288−296.

(10) Sui, J. S.; Yan, J. Y.; Liu, D.; Wang, K.; Luo, G. S. Continuous synthesis of nanocrystals via flow chemistry technology. *Small* **2020**, *16*, No. 190282.

(11) Suryawanshi, P. L.; Gumfekar, S. P.; Bhanvase, B. A.; Sonawane, S. H.; Pimplapure, M. S. A review on microreactors: Reactor fabrication, design, and cutting-edge applications. *Chem. Eng. Sci.* **2018**, *189*, 431−448.

(12) Damilos, S.; Alissandratos, I.; Panariello, L.; Radhakrishnan, A. N. P.; Cao, E. H.; Wu, G. W.; Besenhard, M. O.; Kulkarni, A. A.; Makatsoris, C.; Gavriilidis, A. Continuous citrate-capped gold nanoparticle synthesis in a two-phase flow reactor. *J. Flow Chem.* **2021**, *11*, 553−567.

(13) Volk, A. A.; Epps, R. W.; Abolhasani, M. Accelerated development of colloidal nanomaterials enabled by modular microfluidic reactors: Toward autonomous robotic experimentation. *Adv. Mater.* **2021**, *33*, No. 2004495.

(14) Saldanha, P. L.; Lesnyak, V.; Manna, L. Large scale syntheses of colloidal nanomaterials. *Nano Today* **2017**, *12*, 46−63.

(15) van Embden, J.; Chesman, A. S. R.; Jasieniak, J. J. The heat-up synthesis of colloidal nanocrystals. *Chem. Mater.* **2015**, *27*, 2246−2285.

(16) Quinson, J.; Jensen, K. M. Ø. From platinum atoms in molecules to colloidal nanoparticles: A review on reduction, nucleation and growth mechanisms. *Adv. Colloid Interface Sci.* **2020**, *286*, No. 102300.

(17) Quinson, J.; Neumann, S.; Wannmacher, T.; Kacenauskaite, L.; Inaba, M.; Bucher, J.; Bizzotto, F.; Simonsen, S. B.; Kuhn, L. T.;

Bujak, D.; et al. Colloids for catalysts: A concept for the preparation of superior catalysts of industrial relevance. *Angew. Chem. Int. Ed.* **2018**, *57*, 12338−12341.
(18) Losch, P.; Huang, W. X.; Goodman, E. D.; Wrasman, C. J.; Holm, A.; Riscoe, A. R.; Schwalbe, J. A.; Cargnello, M. Colloidal nanocrystals for heterogeneous catalysis. *Nano Today* **2019**, *24*, 15−47.
(19) Marbella, L. E.; Millstone, J. E. NMR techniques for noble metal nanoparticles. *Chem. Mater.* **2015**, *27*, 2721−2739.
(20) Mateo, J. M.; de la Hoz, A.; Uson, L.; Arruebo, M.; Sebastian, V.; Gomez, M. V. Insights into the mechanism of the formation of noble metal nanoparticles by *in situ* NMR spectroscopy. *Nanoscale Adv.* **2020**, *2*, 3954−3962.
(21) Handwerk, D. R.; Shipman, P. D.; Whitehead, C. B.; Ozkar, S.; Finke, R. G. Mechanism-enabled population balance modeling of particle formation en route to particle average size and size distribution understanding and control. *J. Am. Chem. Soc.* **2019**, *141*, 15827−15839.
(22) Wuithschick, M.; Birnbaum, A.; Witte, S.; Sztucki, M.; Vainio, U.; Pinna, N.; Rademann, K.; Emmerling, F.; Kraehnert, R.; Polte, J. Turkevich in new robes: Key questions answered for the most common Gold nanoparticle synthesis. *ACS Nano* **2015**, *9*, 7052−7071.
(23) Turkevich, J.; Stevenson, P. C.; Hillier, J. A study of the nucleation and growth processes in the synthesis of colloidal gold. *Discuss. Faraday Soc.* **1951**, *11*, 55−57.
(24) Hiramatsu, H.; Osterloh, F. E. A simple large-scale synthesis of nearly monodisperse gold and silver nanoparticles with adjustable sizes and with exchangeable surfactants. *Chem. Mater.* **2004**, *16*, 2509−2511.
(25) Quinson, J.; Bucher, J.; Simonsen, S. B.; Kuhn, L. T.; Kunz, S.; Arenz, M. Monovalent Alkali Cations: Simple and Eco-Friendly Stabilizers for Surfactant-Free Precious Metal Nanoparticle Colloids. *ACS Sustainable Chem. Eng.* **2019**, *7*, 13680−13686.
(26) Bizzotto, F.; Quinson, J.; Zana, A.; Kirkensaard, J. J. K.; Dworzak, A.; Oezaslan, M.; Arenz, M. Ir nanoparticles with ultrahigh dispersion as oxygen evolution reaction (OER) catalysts: synthesis and activity benchmarking. *Catal. Sci. Technol.* **2019**, *9*, 6345−6356.
(27) Quinson, J.; Kacenauskaite, L.; Bucher, J.; Simonsen, S. B.; Kuhn, L. T.; Oezaslan, M.; Kunz, S.; Arenz, M. Controlled synthesis of surfactant-free water-dispersible colloidal platinum nanoparticles by the Co4Cat process. *ChemSusChem* **2019**, *12*, 1229−1239.
(28) Quinson, J.; Kacenauskaite, L.; Schroder, J.; Simonsen, S. B.; Kuhn, L. T.; Vosch, T.; Arenz, M. UV-induced syntheses of surfactant-free precious metal nanoparticles in alkaline methanol and ethanol. *Nanoscale Adv.* **2020**, *2*, 2288−2292.
(29) Bizzotto, F.; Quinson, J.; Schröder, J.; Zana, A.; Arenz, M. Surfactant-free colloidal strategies for highly dispersed and active supported IrO_2 catalysts: Synthesis and performance evaluation for the oxygen evolution reaction. *J. Catal.* **2021**, *401*, 54−62.
(30) Wakisaka, T.; Kusada, K.; Yamamoto, T.; Toriyama, T.; Matsumura, S.; Ibrahima, G.; Seo, O.; Kim, J.; Hiroi, S.; Sakata, O.; et al. Discovery of face-centred cubic Os nanoparticles. *Chem.-Commun.* **2020**, *56*, 372−374.
(31) Hirai, H.; Nakao, Y.; Toshima, N. Preparation of colloidal transition-mtals in polymers by reduction with alcohols or ethers. *J. Macromol. Sci. Chem.* **1979**, *13*, 727−750.
(32) Pitto-Barry, A.; Perdigao, L. M. A.; Walker, M.; Lawrence, J.; Costantini, G.; Sadler, P. J.; Barry, N. P. E. Synthesis and controlled growth of osmium nanoparticles by electron irradiation. *Dalton Trans.* **2015**, *44*, 20308−20311.
(33) Lim, C. S.; Sofer, Z.; Toh, R. J.; Eng, A. Y. S.; Luxa, J.; Pumera, M. Iridium- and osmium-decorated reduced graphenes as promising catalysts for hydrogen evolution. *ChemPhysChem* **2015**, *16*, 1898−1905.
(34) Lam, V. W. S.; Gyenge, E. L. High-performance osmium nanoparticle electrocatalyst for direct borohydride PEM fuel cell anodes. *J. Electrochem. Soc.* **2008**, *155*, B1155−B1160.
(35) Danilovic, N.; Subbaraman, R.; Chang, K.-C.; Chang, S. H.; Kang, Y. J.; Snyder, J.; Paulikas, A. P.; Strmcnik, D.; Kim, Y.-T.; Myers, D.; et al. Activity-stability trends for the oxygen evolution reaction on monometallic oxides in acidic environments. *J. Phys. Chem. Lett.* **2014**, *5*, 2474−2478.
(36) Jiang, K.; Chen, Z. H.; Meng, X. B. CuS and Cu_2S as cathode materials for lithium batteries: A review. *ChemElectroChem* **2019**, *6*, 2825−2840.
(37) Rui, X. H.; Tan, H. T.; Yan, Q. Y. Nanostructured metal sulfides for energy storage. *Nanoscale* **2014**, *6*, 9889−9924.
(38) Guo, M. R.; Law, W. C.; Liu, X.; Cai, H. X.; Liu, L. W.; Swihart, M.; Zhang, X. H.; Prasad, P. N. Plasmonic semiconductor nanocrystals as chemical sensors: Pb^{2+} Quantitation via aggregation-induced plasmon resonance shift. *Plasmonics* **2014**, *9*, 893−898.
(39) Wang, X. L.; Ke, Y. J.; Pan, H. Y.; Ma, K.; Xiao, Q. Q.; Yin, D. Q.; Wu, G.; Swihart, M. T. Cu-deficient plasmonic $Cu_{2-x}S$ nanoplate electrocatalysts for oxygen reduction. *ACS Catal.* **2015**, *5*, 2534−2540.
(40) Cava, R. J.; Reidinger, F.; Wuensch, B. J. Mobile ion disribution and anharmonic thermal motion in fast ion conducting Cu_2S. *Solid State Ionics* **1981**, *5*, 501−504.
(41) Mathiesen, J. K.; Quinson, J.; Dworzak, A.; Vosch, T.; Juelsholt, M.; Kjaer, E. T. S.; Schroder, J.; Kirkensgaard, J. J. K.; Oezaslan, M.; Arenz, M.; et al. Insights from In Situ Studies on the Early Stages of Platinum Nanoparticle Formation. *J. Phys.Chem.Lett.* **2021**, *12*, 3224−3231.
(42) Wu, S. Y.; Li, M. R.; Sun, Y. G. *In situ* synchrotron X-ray characterization shining light on the nucleation and growth kinetics of colloidal nanoparticles. *Angew. Chem., Int. Ed.* **2019**, *58*, 8987−8995.
(43) De Souza, C. D.; Nogueira, B. R.; Rostelato, M. Review of the methodologies used in the synthesis gold nanoparticles by chemical reduction. *J. Alloys Compd.* **2019**, *798*, 714−740.
(44) Liz-Marzán, L. M.; Kagan, C. R.; Millstone, J. E. Reproducibility in nanocrystal synthesis? Watch out for impurities! *ACS Nano* **2020**, *14*, 6359−6361.
(45) Quinson, J.; Mathiesen, J. K.; Schroder, J.; Dworzak, A.; Bizzotto, F.; Zana, A.; Simonsen, S. B.; Kuhn, L. T.; Oezaslan, M.; Jensen, K. M. O.; et al. Teaching old precursors new tricks: Fast room temperature synthesis of surfactant-free colloidal platinum nanoparticles. *J. Colloid Interface Sci.* **2020**, *577*, 319−328.
(46) Quinson, J.; Neumann, S.; Kacenauskaite, L.; Bucher, J.; Kirkensgaard, J. J. K.; Simonsen, S. B.; Kuhn, L. T.; Zana, A.; Vosch, T.; Oezaslan, M.; et al. Solvent-Dependent Growth and Stabilization Mechanisms of Surfactant-Free Colloidal Pt Nanoparticles. *Chem.-Eur. J.* **2020**, *26*, 9012−9023.
(47) Kalinin, S. V.; Sumpter, B. G.; Archibald, R. K. Big-deep-smart data in imaging for guiding materials design. *Nat. Mater.* **2015**, *14*, 973−980.
(48) Mourdikoudis, S.; Pallares, R. M.; Thanh, N. T. K. Characterization techniques for nanoparticles: comparison and complementarity upon studying nanoparticle properties. *Nanoscale* **2018**, *10*, 12871−12934.
(49) Modena, M. M.; Ruhle, B.; Burg, T. P.; Wuttke, S. Nanoparticle characterization: What to measure? *Adv. Mater.* **2019**, *31*, No. 1901556.
(50) Fanizza, E.; Depalo, N.; Clary, L.; Agostiano, A.; Striccoli, M.; Curri, M. L. A combined size sorting strategy for monodisperse plasmonic nanostructures. *Nanoscale* **2013**, *5*, 3272−3282.
(51) Choi, S. H.; An, K.; Kim, E. G.; Yu, J. H.; Kim, J. H.; Hyeon, T. Simple and generalized synthesis of semiconducting metal sulfide nanocrystals. *Adv. Funct. Mater.* **2009**, *19*, 1645−1649.
(52) Hammersley, A. P.; Svensson, S. O.; Hanfland, M.; Fitch, A. N.; Hausermann, D. Two-dimensional detector software: From real detector to idealised image or two-theta scan. *High Press. Res.* **1996**, *14*, 235−248.
(53) Yang, X.; Juhas, P.; Farrow, C. L.; Billinge, S. J. L. xPDFsuite: An End-to-end Software Solution For High Throughput Pair Distribution Function Transformation, Visualization And Analysis,

https://doi.org/10.1021/acsomega.2c00030
ACS Omega 2022, 7, 4714−4721

2015, arXiv:1402.3163v3 [cond-mat.mtrl-sci]. arXiv.org e-Print archive. https://arxiv.org/abs/1402.3163v3.
(54) Juhás, P.; Davis, T.; Farrow, C. L.; Billinge, S. J. L. PDFgetX3: a rapid and highly automatable program for processing powder diffraction data into total scattering pair distribution functions. *J. Appl. Crystallogr.* **2013**, *46*, 560−566.

https://doi.org/10.1021/acsomega.2c00030
ACS Omega 2022, 7, 4714−4721